J Mater Sci (2006) 41:4543–4553
DOI 10.1007/s10853-006-0147-z

TEM and nanomechanical studies on tribological surface modifications formed on roller bearings under controlled lubrication conditions

Manuela Reichelt · Thomas E. Weirich · Joachim Mayer · Thomas Wolf · Jörg Loos · Peter W. Gold · Michel Fajfrowski

Received: 16 February 2006 / Accepted: 21 March 2006 / Published online: 1 July 2006

Abstract The chemical composition and microstructure of reaction layers formed under the presence of lubricants with low wear protection, high wear and fatigue protection, and high wear but low fatigue protection on thrust cylindrical roller bearings made of 100Cr6 steel were analysed by transmission electron microscopy. Thin cross sections prepared by the focused ion beam technique were investigated. The nanomechanical properties of the different tribological layers were analysed by static and dynamic nanoindentation. Our results indicate that wear protection not only relies on the lubricant induced formation of a reaction layer, but also on the properties of the combined system of a reaction layer and an underlying tribomutation layer. The formation and structure of the layer system varies with the chemical nature of the basic oil. Our investigations show that its ability to protect against wear and fatigue strongly depends on the oil viscosity and the additives.

Introduction

Slow running roller bearings often suffer from the absence of a load carrying hydrodynamically lubricating film. Under boundary lubrication conditions, direct contacts of individual roughness points can lead to highly localised energy dissipation with micro-plastic deformation and temperatures (hot spots) up to 700–800 °C. The occurrence of such hot spots leads to surface smoothing by filling existing valleys with sintered reaction products. Another possible process is tribochemical erosion of roughness points [1] or matrix amorphisation [2, 3]. In addition, there is evidence for the formation of a protective oxide layer in the rolling contact zone with a thickness in the range of $1–10^4$ nm. The first report on the formation of such a tribologically protective layer under the influence of a lubricant and an applied tribological load was given by Inacker and co-workers [4]. They determined that the thickness of the tribological protective layers varies between 20 nm and 70 nm by independent measurements with secondary neutral mass spectrometry (SNMS), secondary ion mass spectrometry (SIMS) and focused ion beam (FIB)/scanning electron microscopy (SEM) [5]. Evans et al. [6, 7] have shown the presence of oxide surface layers in sulphur–phosphorus (S–P) additive tribology by transmission electron microscopy (TEM) analysis of FIB cross sections. Scherge et al. [8] investigated the near-surface structure with FIB/SEM techniques and the mechanical properties with dynamic nanoindentation of tribologically induced nanolayers. Towards the underlying matrix, this oxide reaction layer is followed by a tribomutation layer ($d < 10^4$ nm) which consists of a fine crystalline zone [2, 6, 7]. Based upon the present understanding, the composition and properties of the whole layer system depend strongly on the lubricant in use and in particular on the combination of additives [6, 7].

In the present work, we compare the tribological performance of the reaction layers in the investigated model systems and determine their microstructures by analytical

M. Reichelt (✉) · T. E. Weirich · J. Mayer
Central Facility for Electron Microscopy, RWTH Aachen University, Ahornstrasse 55, 52074 Aachen, Germany
e-mail: reichelt@gfe.rwth-aachen.de

T. Wolf · J. Loos · P. W. Gold
Institute for Machine Elements and Machine Design, RWTH Aachen University, Schinkelstrasse 10, 52062 Aachen, Germany

M. Fajfrowski
MTS Systems, Rue Auguste Perret 58, FR-94000 Creteil, France

and high resolution TEM (HRTEM) analysis. The nanomechanical properties were analysed by static and dynamic nanoindentation techniques. By TEM analysis of FIB cross-sectional lamellae of nanoindents produced at a load of 5,000 μN, we were able to perform a detailed investigation of the near surface tribochemical properties.

The samples for the present investigations were selected from different tribological systems, which were obtained by testing standard cylindrical roller thrust bearings in the presence of lubricants with low wear protection (mineral oil with Ca–P–S additives), high wear and fatigue protection (polyalphaolefine oil with ester and P–S additives), as well as high wear but low fatigue protection (mineral oil with Ca–Zn–P–S additives).

Experimental conditions

Tribological systems

The investigations are based on wear experiments [9, 10] which have been carried out in a standardised lubricant and bearing test rig (FE-8, [11]) at a temperature of 80 °C on axial cylinder roller bearings (type 81212) consisting of 15 cylindrical rollers (100Cr6), a polyamid cage (Pa 66), a casing disk (100Cr6) and a shaft disk (100Cr6). Three reference lubricants were chosen which have been well categorised according to the wear protection achieved during the standard tests on the FE-8 test rig (Table 1).

In the wear experiments, the loading conditions were varied systematically by increasing or reducing the applied load in controlled steps or by reducing the number of rollers (Table 2), to determine the threshold level under which the reaction layer is just capable of bearing the load and above which it fails. In this way, the specific load of failure of the tribological system under the given mechanical stress conditions can be determined. The wear criterion was quantitatively assessed by measuring the amount of gravimetrical wear. The failure threshold was defined at a mass loss of the 15 rollers of 10 mg after the wear experiment [12]. If a smaller number of rollers were used, the mass loss is extrapolated to 15 rollers.

Table 1 Lubricants

Classification	Application	Basis oil and additives	Viscosity $V_{40\ °C}$[mm^2/s]
Low wear protection	ATF-oil	Mineral oil Ca, P, S	32
High wear and fatigue protection	Industrial gear oil	PAO/E P, S	100
High wear but low fatigue protection	Motor oil	Mineral oil Zn, Ca, P, S	98

Table 2 Stress level

Load level	Conditions	Contact pressure
1	30 kN, 15 rollers	1,150 MPa
2	50 kN, 15 rollers	1,490 MPa
3	80 kN, 15 rollers (FE8 Standard)	1,890 MPa
4	80 kN, 10 rollers	2,300 MPa
5	80 kN, 5 rollers	3,250 MPa

Methods

The homogeneity, phase and chemical composition of the tribological layers was analysed by conventional TEM, high-resolution TEM, selected area electron diffraction (SAED) and energy-filtered TEM (EFTEM) using an FEI Tecnai F20 instrument. The specimen preparation was performed using an FEI Strata FIB 205 focused ion beam workstation. The information about the surface roughness and micromechanical properties of the reaction layer was determined by a calibrated add-on depth-sensing indentation system (Hysitron TriboScope) on a commercial atomic force microscope (Park Scientific Instruments Autoprobe CP) [13]. The combination of a nanoindenter with an AFM has a symbiotic effect: it extends the capability of the AFM by making nanoindentation experiments with a load and depth resolution (100 nN and 0.2 nm, respectively), and it enables the nanoindentation system to take scanning force images of the sample surface, based on using the same diamond tip for imaging and for indentation [14]. Owing to the small load range of the TriboScope, the investigation of the tribomutation layer and matrix material were additionally performed in a fully calibrated MTS Nanoindenter XP (MTS Systems, Creteil, France) equipped with the continuous stiffness measurement technique (CSM). The system records stiffness data along with load and displacement data dynamically, allowing hardness and modulus to be calculated at every data point acquired during the indentation experiment with a high load and depth resolution (50 nN and <0.01 nm, respectively) [13, 15].

Samples

The chemical and phase composition of the discs and rollers correspond to the specification DIN EN ISO 683-17: 0.93–1.05 wt.% C, 0.15–0.35 wt.% Si, 0.25–0.45 wt.% Mn, 0.025 wt.% S, 1.35–1.60 wt.% Cr, max. 0.10 wt.% Mo and max. 0.050 wt.% Al, as was revealed by previous investigations of a reference sample [16]. The surface near zone of the reference sample was finely crystalline without texture due to the final grinding treatment. The transition zone between this fine crystalline layer and the granular bulk martensite structure is not well defined and the thickness of the fine crystalline zone varies between 50 nm

and 200 nm. All our present investigations were performed on one of the bearing discs of the different tribological systems. The experimental conditions resulted in the following sample properties (see Table 3): The bearing tested with the lubricant with low wear protection was run for 8 h with a contact pressure of 1,150 MPa (load level one) and has already shown wear to failure ($m > 10$ mg). The bearing tested with the lubricant with high wear and fatigue protection was run for 80 h with a contact pressure of 2,300 MPa (load level 4) and satisfied the wear criterion ($m < 10$ mg). The bearing tested with lubricant with high wear but low fatigue protection was run for 80 h at 3,250 MPa ($m < 10$ mg).

For sample preparation the bearing discs were first cut on a Vari/Cut V C-50 (Leco Corporation) low-speed diamond saw in mineral spirits (Buehler) under water-free conditions. Several small pieces suitable for further nanoindentation studies and TEM specimen preparation were obtained. Electron-probe microanalysis (EPMA) measurements proved that the samples can be cleaned with acetone for 30 min in an ultrasonic bath without damaging the reaction layer.

The TEM specimen preparation was performed using dedicated FIB procedures. Prior to sectioning, the reaction layer was protected with a sputtered gold layer and a tungsten coating deposited in the FIB. All lamellae were prepared on the outer track of the bearing disc, where the slip contribution is positive. Only the TEM investigations of the bearing disc with lubrication with low wear protection were carried out on the inner and outer tread because of the visible wear on the inner tread.

Results and discussion

Microstructural investigations

System I: low wear protection

First the results obtained on the bearing disc with lubrication with low wear protection will be discussed. The lubrication was based on a mineral oil with Ca-, S- and P-additives. Fig. 1 shows a bright-field (BF) image of the wear region on the inner tread of the bearing disc. After failure in this system the reaction layer is discontinuous and consists of rather massive pieces of deposited oxide. The presence of these pieces is revealed by the coloured tracks on the inner tread of the bearing. Energy dispersive X-ray (EDX) spectroscopy analysis on the reaction layer pieces revealed iron and oxygen as main components and chlorine, silicon, sulphur, potassium, chromium, aluminium, calcium and phosphor as additional elements. SAED analysis showed the multi-crystalline nature of these phases. TEM bright-field image analysis gave no evidence for the formation of a fine crystalline zone underneath the discontinuous reaction layer.

Table 3 Experimental conditions used in the tribological tests

Oil classification	Load level [MPa]	Runtime [h]	breakdown
Low wear protection	1 (1,150)	8	Yes, $m > 10$ mg
High wear and fatigue protection	4 (2,300)	80	No, $m < 10$ mg
High wear but low fatigue protection	4 (2,300)	80	No, $m < 10$ mg
	5 (3,250)	80	No, $m < 10$ mg

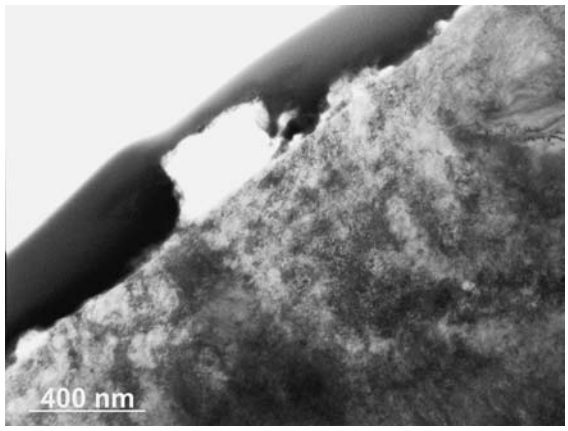

Fig. 1 TEM-BF cross-section image of the wear region on the surface of the bearing disc with lubrication with low wear protection. The dark region on the top represents the gold protection layer. Bright adhesions to the surface are the polycrystalline remnants of the reaction layer. The surface near zone shows no indication for the formation of a fine crystalline tribomutation layer

The dark-field (DF) image displayed in Fig. 2 shows the mostly intact reaction layer (bright layer) on the outer tread of the same bearing disc. The thickness value of the reaction layer is 0–100 nm. Detailed inspection of BF images revealed that the reaction layer apparently exhibits pores inside. According to Holweger [17] these pores can be interpreted as inclusions of additives dissolved in some basis oil. By TEM measurements one cannot make a detailed statement about the consistency of the solution in the pores. However, SIMS and SNMS investigation on similar tribological systems revealed a high concentration of carbon in the reaction layer [4]. This is an indication for the inclusion of a high lubricant content in the reaction layer of this system. Underneath the reaction layer a plastic deformation zone consisting of fine crystals with a high defect density can be identified. This tribomutation layer is about 400 nm thick and shows strong texture. The transition region between tribomutation layer and matrix is not well defined, as can be expected from the gradual decrease

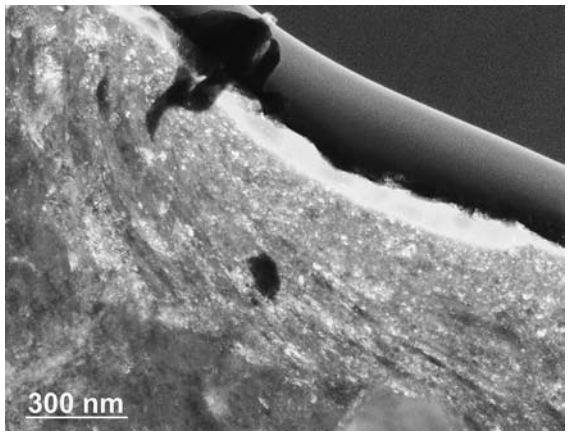

Fig. 2 TEM-DF cross-section image of the outer tread of the bearing disc with lubrication with low wear protection. The bright area represents the reaction layer. Near the surface a fine crystalline tribomutation layer with strong texture has been formed

of plastic deformation as a function of the distance from the surface.

An EFTEM analysis verified that Fe and O are the main constituents forming the solid reaction layer (Fig. 3). Additional EDX analysis revealed the presence of small amounts of several additive-elements like calcium, potassium and sulphur. An analysis of HRTEM micrographs proved that the solid reaction layer is formed by amorphous iron oxide with embedded nanocrystalline particles, which could be identified as Fe_2O_3. The chemical composition and thickness are in accordance with the results obtained by Evans et al. [6, 7] in investigations of antiwear (AW) surface-layers formed under the presence of mineral oil with sulphur–phosphorus (S–P) additives. Like in our experiments, they also observed the presence of filled pores inside the reaction layers.

System II: high wear but low fatigue protection

In the tribological system with lubrication with high wear but low fatigue protection, the reaction layer shows an increasing average thickness with increasing load. The layer formed at a 2,300 MPa load has a median thickness value of about 40 nm (Fig. 4) and the layer formed at 3,250 MPa of about 70 nm (Fig. 5). Both reaction layers show pores inside (see Fig. 4) which can also be interpreted as inclusions of lubricant. HRTEM micrographs revealed that the oxide phase forming the reaction layer is nanocrystalline with an amorphous layer of about 4-nm thickness on the top (Fig. 6). The interface between the matrix and the reaction layer shows a well-defined crystalline transition zone. EDX analysis verified the presence of calcium, zinc, phosphor and oxygen as main constituents of the reaction layer.

More detailed information on the chemical composition of the layer system was obtained by energy-loss spectroscopy in our EFTEM. Energy-filtered images were acquired in the energy-loss range 250–750 eV and subsequently a

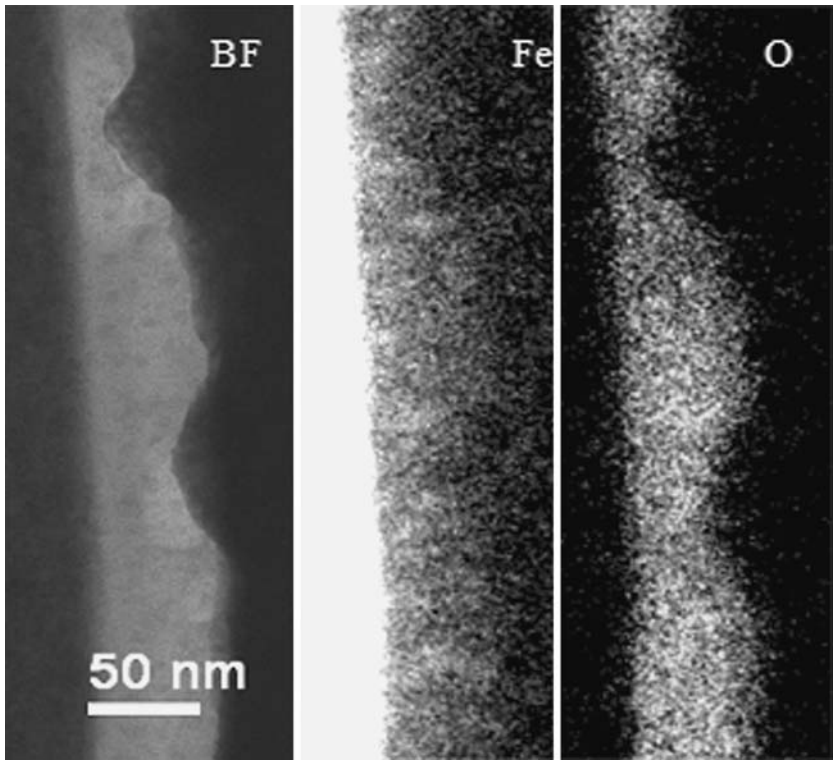

Fig. 3 EFTEM images of the reaction layer formed by lubrication with low wear protection. Left: BF-image, middle: iron map, and right: oxygen map

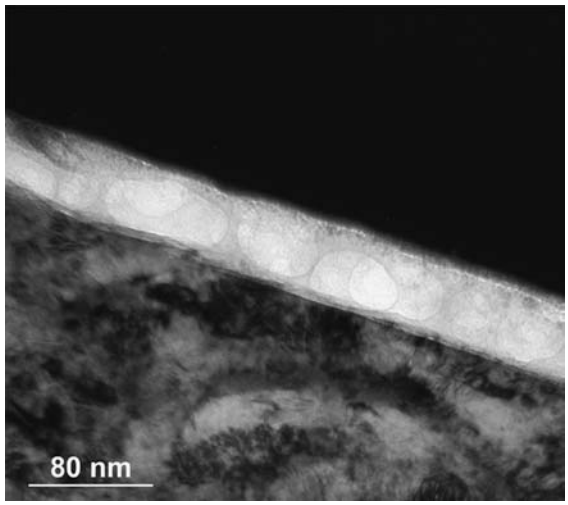

Fig. 4 TEM-BF cross-section image of the system with lubrication with high wear but low fatigue protection tested at load-level 4. The bright layer is the reaction layer which consists of a solid crystalline phase incorporating a large amount of filled pores

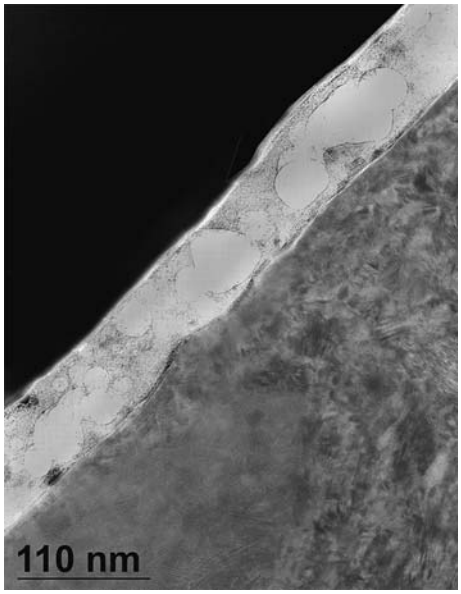

Fig. 5 TEM-BF cross section image of the system with lubrication with high wear but low fatigue protection obtained at load-level 5. The bright layer is the reaction layer

spectrum line profile across the layer system was extracted from these data. Details of the technique are described in [18]. A spectrum line profile crossing the interface matrix-reaction layer (from behind) across the reaction layer itself to the surface (in front) is shown in Fig. 7. The edges corresponding to calcium, oxygen and iron are visible in this energy-loss range, whereas the edge energy of phosphorus (132 eV) is outside of the interval shown. These investigations verified that the reaction layer mainly consists of calcium phosphate. The iron peak intensity almost

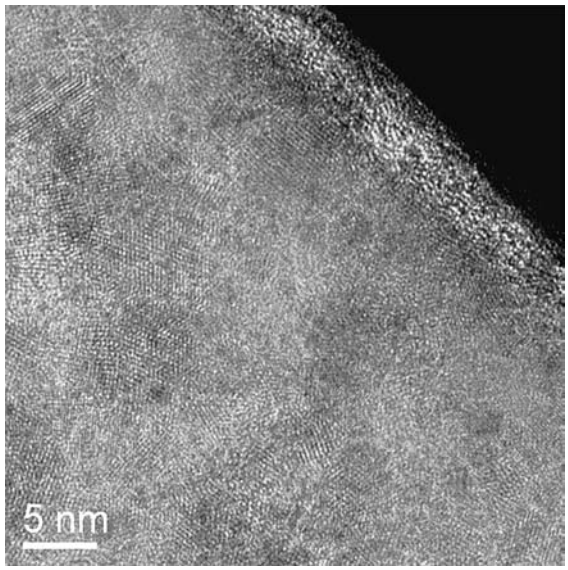

Fig. 6 HRTEM cross-section image of the system with lubrication with high wear but low fatigue protection obtained at load-level 5. The image reveals the fine crystalline nature of the reaction layer with a thin amorphous layer deposited on the top

vanishes from the matrix to the reaction layer, but is also slightly present on the top surface of the reaction layer. In addition, changes in peak morphology are an indication of different bonding states of the iron, i.e. metallic in the matrix and oxidic in the surface layer. EDX maps show that a slight zinc accumulation exists at the interface between reaction layer and matrix.

The thickness of the reaction layer formed by the lubricant with high wear but low fatigue protection is

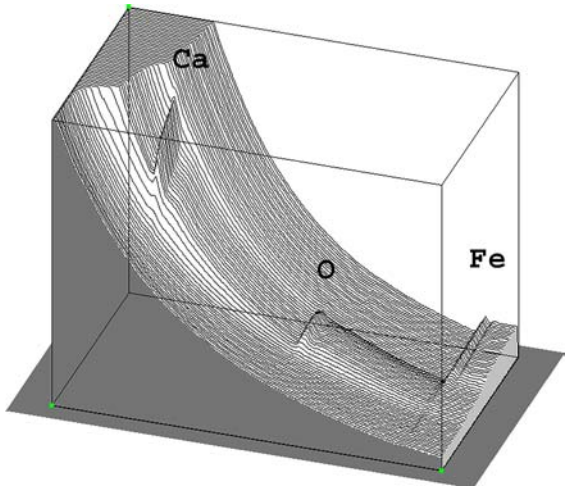

Fig. 7 EELS-data collected from the layer system, starting in the matrix (in the track) across the reaction layer (in the middle) to the top (in front) in the energy range of 250–750 eV. It is clearly visible that the reaction layer contains Ca and O, whereas the third major constituent, P, is not visible because the corresponding edges are outside of the energy loss range investigated in the experiment. A slight Fe accumulation can be seen in the front, i.e. towards the top surface

similar to the one discussed first, but with a rather complex structure which was only revealed by the different analytical TEM methods and HRTEM. The latter reaction layer is a deposition of oxidation products of the additive elements with inclusions of lubricant contents, but with a crystalline transition between matrix and layer. This is in contrast to the case discussed first, which was mainly based on oxidation of the matrix element, iron. So, the modification of the additives thus changes the structure and chemical composition of the reaction layer, in particular at the transition between matrix and layer. The thickness of the tribomutation layer is in both cases about 200 nm and seems to be independent of the load.

System III: high wear and fatigue protection

In the system with lubrication with high wear and fatigue protection, substantial differences to the first two cases were found in our studies. As can be seen in Fig. 8, the reaction layer exhibits an average thickness value of only 6 nm. In this case, the lubricant was based on a polyalphaolefine with ester, in contrast to the other lubricants that were based on mineral oil, but also contained S- and P-additives. HRTEM revealed that the thin amorphous layer also contained nanocrystalline particles inside. Fourier transformation of the HRTEM images proved that the nanocrystalline particles also consist of Fe_2O_3. The effects of the strong plastic deformation on the original microstructure are visible in a subsurface tribomutation layer 200 nm thick. In this fine crystalline layer we also found a chromium accumulation. There is reason to assume that this is due to finely dispersed chromium carbides in a surface near zone, which accumulate under the abrasive tribological conditions. SAED analysis verified the presence of non-metallic inclusion of the type $Cr_{23}C_6$. In this case, the transition to the matrix is well defined.

An EFTEM analysis proved that Fe and O are the main constituents forming the reaction layer of the system with lubrication with high wear and fatigue protection. The EDX analysis revealed the presence of small amounts of several additive elements like sulphur and phosphorus (Fig. 9).

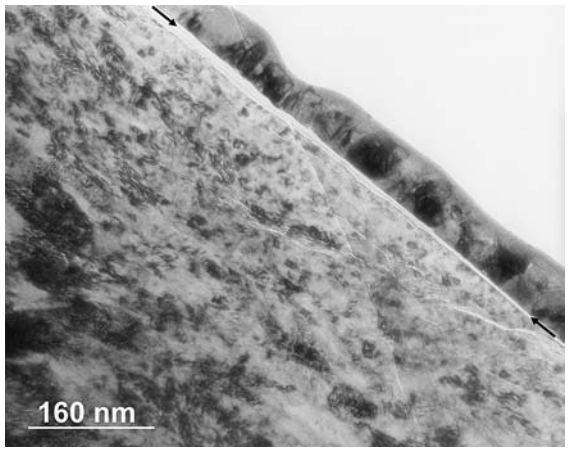

Fig. 8 TEM-BF cross-section image of the system with lubrication with high wear and fatigue protection. The bright line (arrowed) represents the ultra-thin reaction layer between the dark gold protection layer and the fine crystalline tribomutation layer. The cracks are artefacts produced during preparation

Additionally, the non-load carrying areas of the system with lubrication with high wear protection were investigated. There we also found an amorphous iron oxide, but with a higher carbon concentration and without nanocrystalline particles. The oxide layer also exhibits a high variation in the thickness.

From the composition, it can be expected that both mineral-oil-based systems show the formation of the same kind of reaction layer, but in reality only the thickness of the reaction layer is similar. The system with lubrication with high wear but low fatigue protection (system II) exhibits a layer with a rather complex structure which was only revealed by the different analytical TEM methods including HRTEM. Our results have shown that the latter reaction layer forms by deposition of oxidation products of the additives elements with some inclusions of lubricant contents. In contrast, the system with lubrication with low wear protection (system I), forms a layer which is mainly based on oxidation of the matrix element, i.e. iron. Finally, the reaction layer of the system with lubrication with high wear and fatigue protection is ultra thin, and mostly

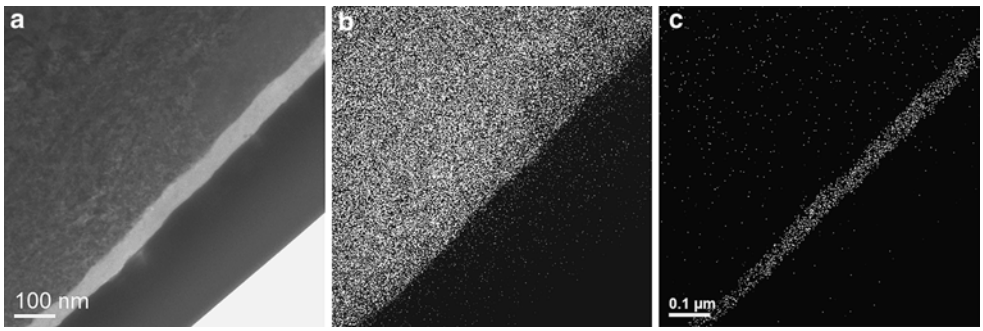

Fig. 9 EFTEM images of the reaction layer formed by lubrication with high wear and fatigue protection. Left: BF-image, middle: iron map, and right: oxygen map

consists of amorphous iron oxide. According to Lim and Ashby [19] the oxidation of the matrix elements can be differentiated in severe or even melt oxidation for the system with lubrication with low wear protection and mild oxidational wear, which we observe for the system with lubrication with high wear and fatigue protection. Nevertheless, the melt oxidation layer contained also oxidation products of the additive elements. Whether this indicates the initial stages in the formation of a reaction layer by additive elements, which then is suppressed by melt oxidation of matrix elements during the wear process, will have to be clarified in further investigations. Our investigations show that modification of the additives also changes the structure and chemical composition of the reaction layer.

The thickness of the tribomutation layer of the systems with high wear protection is in both cases about 200 nm and seems to be independent of the load. While the transition from the reaction layer to the tribomutation layer of the system with high wear and fatigue protection is well defined and shows a sharp interface, the systems based on mineral oil lubrication show a distinct thickness variation or waviness. The latter can be evidence for tribochemical erosion of roughness points.

AFM investigations

In atomic force microscopy (AFM) investigations, we found evidence for substantial surface smoothing under the tribological load in large regions between the furrows induced by grinding. The surface roughness of the systems with lubrication with low wear and high wear but low fatigue protection is about 6 nm. Both samples exhibit a micro ripple content of the surface that may be related to the oil-filled pores. For the system with high wear protection, a surface roughness of only 2 nm and without ripple was found. In comparison, a polished reference sample has a roughness of about 1.2 nm and the surface roughness of an unpolished reference sample amounts to about 40 nm.

It is well known that the asperity–asperity contact results in surface smoothing. In our studies, the amount of smoothing is strongly dependent on the type of lubricant.

Nanoindentation experiments

The nanomechanical properties of the different tribological layers were investigated by means of the static and dynamic nanoindenter. The experiments with the static TriboScope were made with the load variation method (LVM) [14] and a maximum load of 150 μN and 20 μN with a blunt Berkovich Indenter (radius of curvature of the tip 160 nm). With this method, one can measure the properties of the sample in the as-formed condition of the layers. Each data point or curve obtained in the corresponding experiments represents the mean of at least 10 and a maximum of 50 measurements. The nanomechanical properties of the bulk material were measured by using the static indentation method with a Berkovich tip and maximum load of 9,500 μN and 8,000 μN, respectively. For correction and calculation of the obtained load–displacement curve, we used the different methods of the software IndentAnalyser (ASMEC) package based on the Oliver–Pharr method [20–22]. The dynamic Nanoindenter XP measurements were performed with a Berkovich tip (tip curvature < 10 nm) and the maximum displacement into the surface was 400 nm (displacement control). The continuous stiffness measurement technique provides the opportunity to measure the mechanical properties and to characterise the resistance to plastic penetration P/S^2 [14] of the reaction layer, the fine crystalline zone and the matrix to determine the characteristic differences between the low wear and fatigue as well as the high wear protection systems. At least nine indentations were performed for each tribological system and averaged. Results were analysed with the well known Oliver–Pharr method [20–22] using the TestWorks Software.

As a result of the final surface treatment, the untested, polished reference sample is around 2 GPa harder than the tribologically tested samples. The reference sample exhibits a maximum hardness at a displacement into the surface of about 50 nm (Fig. 10). Scherge et al. [8] assume that the grinding process introduces internal stresses and leads to strengthening due to cold working, resulting in higher hardness. The sample with lubrication with low wear protection showed a maximum hardness zone located nearer to the surface (see Fig. 10). In contrast, the sample with lubrication with high wear and fatigue protection had the same appearance of the hardness curves, but at a value of 2 GPa lower than the reference samples. The most significant difference in the appearance of the hardness curve

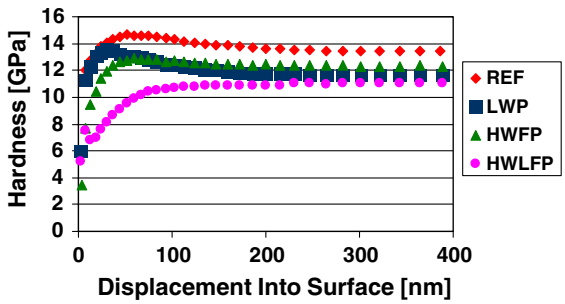

Fig. 10 Comparison of hardness determined at a maximum displacement into the surface of 400 nm with a Berkovich indenter. Abbreviations and experimental conditions are: REF: Reference sample, LWP: Reference oil with low wear protection [mineral oil, Ca–P–S additives], HWFP: Reference oil with high wear and fatigue protection [PAO/E, P–S additives], HWLFP: Reference oil with high wear but low fatigue protection [mineral oil, Ca–Zn–P–S additives]

is shown by the sample with lubrication with high wear, but low fatigue protection, for which no maximum hardness peak and the lowest hardness values of all are found. We conclude that for this system the hardness values of the first 100 nm are influenced strongly by the thick reaction layer with low hardness value.

Figure 11 shows the influence of the tribological treatments on the resistance to plastic deformation. One major advantage of using this technique is that it does not require a detailed knowledge of the indenter geometry. An interesting consequence of this is that the technique is not so much sensitive to changes in hardness but is sensitive to changes in elastic modulus [13]. The reference sample, the sample with high wear and fatigue protection, and the sample with low wear protection exhibit a very similar depth-dependent resistance to plastic penetration, even though the hardness values are significantly different. Compared to the other tribological systems, the sample with lubricant with high wear but low fatigue protection has a lower resistance to plastic penetration, due to a lower hardness value for displacements into the surface of up to about 300 nm. Independent of the presence of the reaction layer, the surface near zone, in the 100–300 nm range, got softer with a higher plasticity. It can be assumed that this effect is coupled to the low fatigue protection.

In another set of static (Triboscope) experiments applying a Berkovich indenter and loads of 9,500 μN and 8,000 μN, the nanomechanical properties on a cross-sectioned, polished reference sample were investigated. The average of the 50 measurements resulted in a Modulus of 230 Gpa ± 15 GPa (standard deviation) and a hardness value of 8.2 Gpa ± 0.6 GPa of the bulk material. A comparison with the hardness curves shown in Fig. 10 indicates that these hardness values are far away from those of the bulk material. This suggests that the range of the influence of the manufactured surface hardening, see DIN EN ISO 683-17, is greater than the maximum displacement into surface of 400 nm.

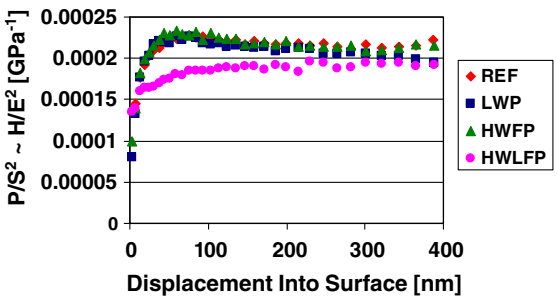

Fig. 11 Comparison of resistance to plastic deformation H/E^2 determined at a maximum displacement into the surface of 400 nm with a Berkovich indenter. Abbreviations and experimental conditions see Fig. 10

In further static investigations (Fig. 12), we compared the nanomechanical properties of the fine crystalline zone on an untested, polished reference sample with the tribomutation layer of the system with lubrication with high wear and fatigue protection, for which we were able to remove the ultra-thin reaction layer. On the other hand, the indentation modulus of the systems with lubrication of low wear and high wear but low fatigue protection was measured including the reaction layer, because we were unable to remove the reaction layer in these systems.

The Young's modulus of the reference sample and of a sample with lubrication with high wear and fatigue protection was determined with a load of 150 μN and the results are similar to those of dynamic measurements. In contrast, the indentation moduli of the systems with lubrication with low wear, as well as high wear but low fatigue protection are substantially lower, with a mean value of 150 GPa, see Fig. 12. The indentation modulus is a compound modulus of the reaction layer and the tribomutation layer. This fact also applies to the hardness values. We can thus only explain the results in these two systems with the presence of a really soft reaction layer because we have already shown that the properties of the underlying tribomutation layer are very similar in all systems.

For determination of Young's modulus of the ultra-thin reaction layer, measurements were performed with the minimum load of 20 μN. For this purpose, it is necessary to acquire reproducible, fully elastic load–displacement curves, from which the Young's modulus can be calculated by elastic fit (IndentAnalyser).

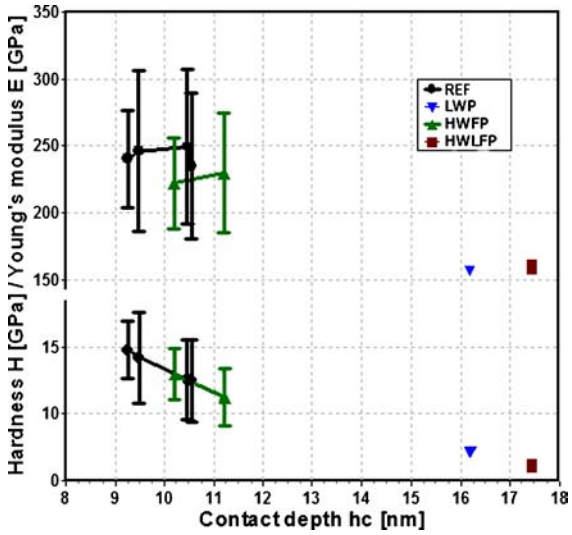

Fig. 12 Comparison of hardness and Young's modulus measured at a maximum load of 150 μN with a Berkovich indenter. The ordinate axis is discontinuous—note the different scale. Abbreviations see Fig. 10

The results indicate that the compound modulus of the amorphous oxide layer and the underlying fine crystalline tribomutation layer of the sample with lubrication with high wear and fatigue protection has a value of approximately 130 GPa. By using the elastic fit method described above, it could be determined that the amorphous oxide layer has a rather low Young's modulus of only 46 GPa, calculated with an assumed Poisson's ratio of 0.27, which was also used for the matrix. Fig. 13 shows that the fully elastic experimental load–displacement data of the sample with lubrication with high wear and fatigue protection are in good agreement with finite element method (FEM) simulations for a two-layer system evaluated under the assumption of a spherical indenter (indenter radius 160 nm).

To understand the influence of these very thin reaction layers and the underlying tribomutation layer on the tribological properties, we performed TEM studies on nanoindents cross-sectioned with the FIB technique. We investigated the system formed by the lubricant with high wear and fatigue protection in comparison to a polished reference sample. For the experiments arrays of indents were prepared and FIB lamellae were cut always covering three indents.

For the indents of both systems investigated, the load–depth data recorded with a maximum load of 5,000 μN were identical and also the resulting hardness values of nominally 8.5 GPa. The Young's moduli showed slight differences with 224 GPa for the polished reference sample and 208 GPa for the system formed with lubrication with high wear and fatigue protection.

In overview images the indents look similar and both samples have pile-ups on either side of the indents. The sample tested with lubrication with high wear and fatigue protection exhibits the known reaction layer on the top surface, and underneath the fine crystalline tribomutation layer. The reaction layer and the fine crystalline zone are penetrated by the indents (Fig. 14). The polished reference sample does not show structural modifications compared with the matrix and the surface is really smooth. At higher magnification, distinct differences can be noticed in the two systems. Whereas Fig. 14 shows a well-defined indent for the system with lubrication with high wear and fatigue protection, Fig. 15 displays an indent with rather diffuse boundaries in the polished reference sample. At all three indents within the FIB lamella of the polished reference sample, substrate material was adhering to the indenter tip during the unloading treatment. As a consequence, the polished reference sample exhibits pile-ups with clearly visible glide planes, see Fig. 15. These results clearly show that the reaction layer formed during the tribological tests substantially reduces the adhesive properties of the matrix material and acts as a solid lubricant in direct interaction with the counterpart material.

In addition, the results make it possible to deduce the response of the system when subjected to the impact of hard particles like chromium carbides of the counterpart material, which have a similar size than the indents. In this case, the reaction layer prevents adhesion and the fine crystalline zone of the tribomutation layer adsorbs the energy of the plastic deformation.

Conclusions

In the present work, we have compared the tribological performance of three different bearing/lubricant systems that are characterised by the presence of a tribological layer

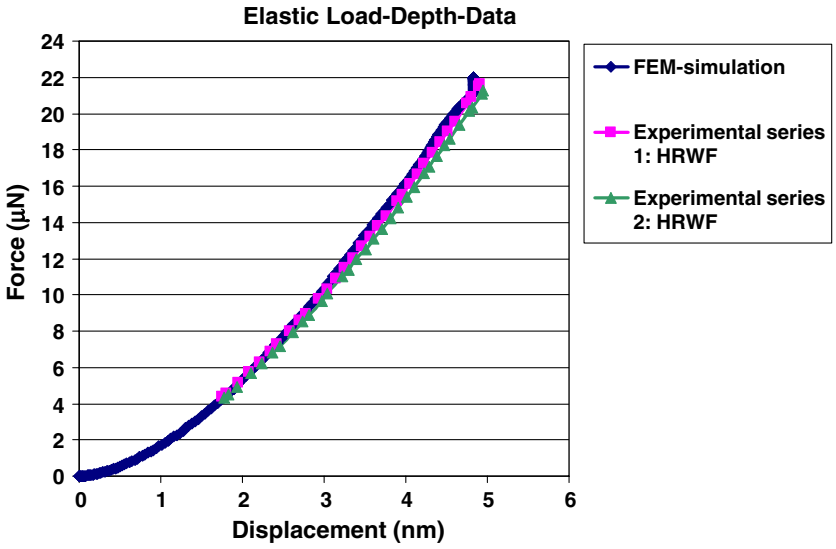

Fig. 13 Comparison of two series of elastic load depth data measured at a maximum load of 20 μN with a Berkovich indenter (tip rounding 160 nm) with finite element simulations for a two-layer model with a starting value of Young's modulus for the reaction layer of 46.6 GPa and the substrate of 205 GPa

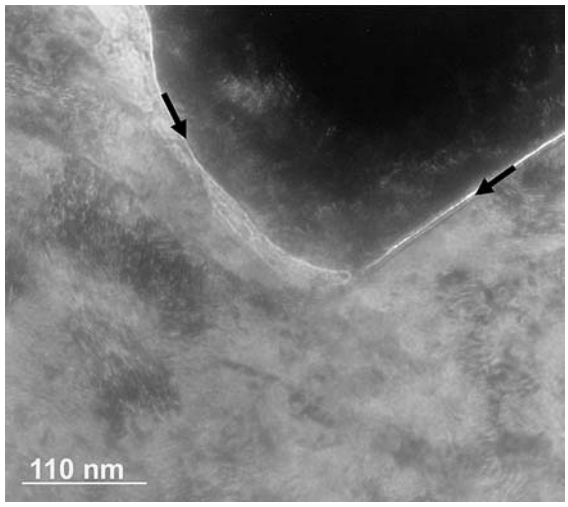

Fig. 14 TEM-BF cross-section image of an indent produced with a maximum load of 5,000 μN with a Cube Corner indenter in the bearing disc with lubrication with high wear and fatigue protection. The dark region is part of the gold protection layer. The bright line (arrowed) represents the amorphous reaction layer

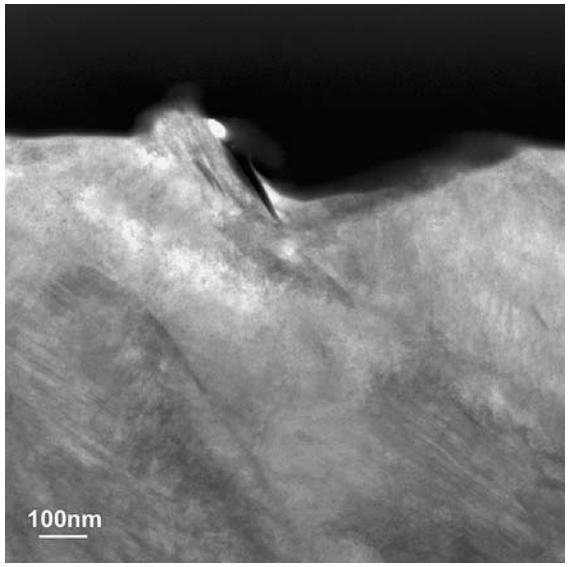

Fig. 15 STEM-DF cross-section image of an indent measured at a maximum load of 5,000 μN with a Cube Corner indenter inside the polished reference sample: The dark area represents the gold protection layer

system consisting of a reaction layer and a tribomutation layer. For this purpose, we applied TEM analysis to reveal details of the microstructure and depth-sensing nanoindentation systems to access the nanomechanical properties. By a combination of thorough TEM analysis of FIB-prepared cross-section lamella with nanoindentation measurements, we were able to perform a detailed investigation of the near-surface properties.

The formation and the morphology of the reaction layers depend strongly on the oil type used for lubrication. Ester-based oils (Type PAO/E) promote the formation of single, iron oxide-based ultra-thin reaction layers with an average thickness of only 6 nm. The corresponding lubricant delivered high wear and fatigue protection, in which the properties of the ultra-thin reaction layer seem to play an important role.

Mineral oil based lubricants cause the formation of much thicker reaction layers with a complex morphology comprising a characteristic porosity. The mineral oil based lubricant with low wear protection only led to the formation of a discontinuous, iron oxide based reaction layer with strongly varying thickness. In contrast, additives in the lubricant with high wear but low fatigue protection caused the formation of a double layer system consisting of a calcium phosphate-based layer with a uniform thickness of about 36 nm or 66 nm, and a thinner amorphous iron oxide layer with an average thickness of 4 nm on the top. In the latter case, the thickness of the final reaction layer showed a significant dependence on the applied load level. Independent of the chemical composition, all reaction layers are much softer and have a lower elastic modulus than the matrix material.

In the matrix underneath the reaction layer, a tribomutation layer forms in all systems, which is characterised by a fine crystalline defect-rich microstructure caused by the heavy plastic deformation. The thickness of the tribomutation layer depends on the amount of wear protection provided by the lubricant and is of the order of 200 nm in the case of high wear protection and of about 400 nm for lubricants with low wear protection. Owing to the defects introduced by mechanical surface finishing the untested reference sample was harder than the tribologically tested samples. The tested samples show no evidence of surface hardening due to tribological treatment; rather the sample with lubricant with high wear but low fatigue protection is significantly softer and exhibits lower resistance to plastic deformation.

The results of our studies give clear evidence that the combined action of the reaction layer and the tribomutation layer controls the tribological properties of the systems investigated. In particular, the TEM studies of cross-sectioned nanoindents revealed that the reaction layer is capable of providing sufficient adhesion protection, even in the case of severe plastic deformation and in the absence of any lubricants. It is also remarkable that, in particular, the ultra-thin reaction layer seems to serve most perfectly for this purpose. Under non-adhesive conditions, the severe plastic deformation under the applied frictional sliding conditions leads to substantial surface smoothing, without causing a hardening effect in the load carrying areas. As a final remark, it should be noted that under the action of the

lubricants with high wear protection, the reaction layer/tribomutation layer system must be rapidly self-reproducing, given that under the applied tribological loads it is impossible to avoid strong local abrasion.

Acknowledgement The authors gratefully acknowledge financial support by the Deutsche Forschungsgemeinschaft (DFG) [GO 684/8-3 and MA 1280/22-1] and the European Commission through the Nanobeams Network of Excellence [FP6-500440-2].

References

1. Uetz H, Foehln J, Sommer K (1989) Antriebstechnik 28:57
2. Meyer K, Kloß H (1993) Reibung und Verschleiß geschmierter Reibsysteme. Expert Verlag, Renningen, Germany
3. Meyer K (1985) Tribologie Schmierungs 5:254
4. Jao TC, Inacker O, Beckmann P, Yatsunani K (2006) In: Esslingen TAE (ed) Proceedings of the 15th International Colloquium on Tribology, Automotive and Industrial Lubrication, Stuttgart, Germany, CD-ROM15-E6
5. Inacker O, Beckmann P (2002) In: Esslingen TAE (ed) Proceedings of the 13th International Collegium of Tribology, Ostfildern, Germany, CD-ROM15-EX
6. Evans RD, More KL, Darragh CV, Nixon HP (2004) Tribology Trans 47:430
7. Evans RD, More KL, Darragh CV, Nixon HP (2005) Tribology Trans 48:299
8. Scherge M, Pöhlmann K, Shakhvorostov (2006) Wear 260:433
9. Loos J (2001) ''Leistungsfähige Wälzlager für umweltverträgliche Schmierstoffe durch PVD Verschleißschutzschichten'', PhD thesis, RWTH Aachen University
10. Waldbeck Th (2004) ''Das Viskositätsverhalten und die Schmierfilmbildung von Schmierstoffen in Abhängigkeit von Druck und Temperatur'', PhD thesis, RWTH Aachen University
11. DIN EN ISO 51819-(1–3)
12. DIN 51517
13. Fischer-Cripps AC (2004) Nanoindentation. Springer-Verlag, Berlin, Germany
14. Kunert V (2000) Mechanical properties on nanometer scale and their relations to composition and microstructure, PhD thesis, Max-Planck Institute for Metals Research, University of Stuttgart
15. Bhushan B (2004) Springer handbook of nanotechnology. Springer Verlag, Berlin, Germany, p 701
16. Reichelt M, Weirich Th, Richter S, Aretz A, Mayer J, Wolf Th, Klaas H, Loos J, Gold PW (2005) Tribologie Schmierungs 02:18
17. Holweger W (2006) In: Esslingen TAE (ed) Proceedings 15th International Colloquium on Tribology, Automotive and Industrial Lubrication, Stuttgart, Germany, CD-ROM 15-E3
18. Plitzko JM, Mayer J (1999) Ultramicroscopy 78:207
19. Lim SC, Ashby MF (1987) Acta Metall. 35:1
20. Chudoba T, Richter F (2001) Surf Coat Tech 148:191
21. Oliver WC, Pharr GM (1992) J Mater Res 7:1564
22. Pharr GM, Oliver WC, Brotzen FR (1992) J Mater Res 7:613